Concurring chalcogen- and halogen-bonding interactions in supramolecular polymers for crystal engineering applications

Nicolas Biot and Davide Bonifazi*

[*] Nicolas Biot and Prof. Dr. D. Bonifazi
    School of Chemistry; Cardiff University
    Park Place, CF10 3AT, Cardiff, United Kingdom.
    E-mail: BonifaziD@cardiff.ac.uk

Abstract: The engineering of crystalline molecular solids through the simultaneous combination of distinctive non-covalent interactions is an important field of research as it could allow chemist to prepare materials depicting multiresponsive properties. It is in this contest that, pushed by our will to expand the chemical space of chalcogen-bonding interactions that, in this work we put forward the concept for which chalcogen- and halogen-bonding interactions can be used simultaneously to engineer multicomponent co-crystals. Through the rational design of crystallizable molecules, we prepared chalcogenazolo pyridine scaffold (CGP) modules that, bearing either a halogen-bond acceptor or donor at the 2-position can interact with suitable complementary molecular modules, undergoing formation of supramolecular polymers at the solid state. The recognition reliability of the CGP moiety to form chalcogen-bonded dimers allow the formation heteromolecular supramolecular polymers through halogen-bonding interactions as confirmed by single-crystal X-ray diffraction analysis.

Figure to the table of content.
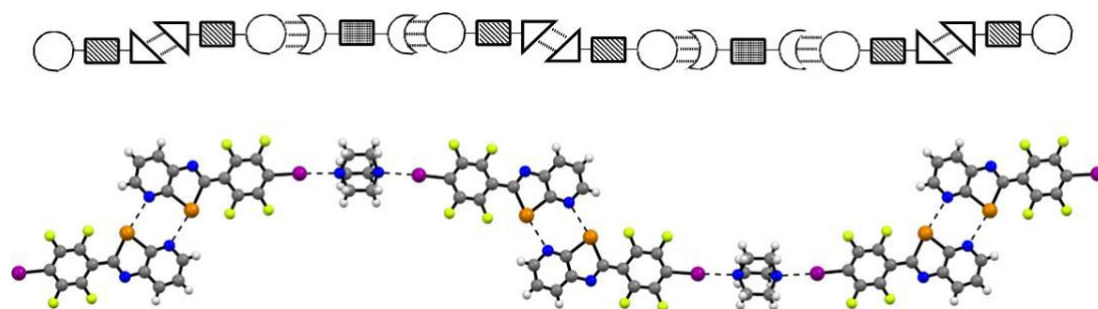
Introduction

The primary aim of supramolecular chemistry is to link molecular chemistry with the construction of thermodynamically-stable architectures of higher complexity through the principle of self-assembly using non-covalent interactions.[1] In this respect, the possibility of simultaneously exploiting multiple interactions[2] can allow chemists to engineer architectures with multiresponsive properties.[3] For example, this is the case of supramolecular polymers,[4] whose monomeric units hold together via highly directional and reversible non-covalent interactions. In a series of instances, it has been shown that multi-responsive materials could be prepared when monomers displaying heterotopic recognition units were used.[5] Another example is that of molecular solids, the functional properties of which enabled through the rational design of crystallizable molecular synthons undergoing programmed non-covalent directional interactions.[6] Typical examples describe the simultaneous of use of H-bonding (HBIs) and metal-coordination interactions.[7]

Beside the classical interactions of the supramolecular toolbox,[8] in the recent years chemists became interested in secondary-bonding interactions (SBIs).[9] The Halogen-bonding interaction (XBI) is the most renowned SBI,[6d, 9b, 10] and its use has been validated in crystal engineering applications,[11] liquid crystals,[12] functional materials,[13] and biochemistry.[14] Structures containing electron-deficient chalcogen atoms can also give rise to SBIs, known as chalcogen-bonding interactions

(EBIs).[15] Recent investigations showed that chalcogen bonds could be used to foster molecular organization in solids,[16] anion recognition and transport,[17] catalysis,[18] biology[19] and self-assembly.[20] While XBIs have been proven to be compatible with HBIs both in crystals[21] and biological systems,[22] the simultaneous expression of EBIs with other interactions has been marginally studied.[23] Recent examples include the formation of wire-like assemblies at the solid state of 1,4-diiodotetrafluorobenzene (**DITFB**) with either 2,1,3-benzoselenadiazole[23a] or diphenyl dichalcogenide.[23c] Ourselve, we recently repored a heteromolecular polymeric chain, in which the monomers are held together through EBIs and XBIs at the solid state.[23b] It is in this context that herein we present a full account on the rational engineering of multicomponent co-crystals through the simultaneous expression of chalcogen- and halogen-SBIs. Building on the recognition persistency of the self-associating chalcogenazolo pyridine scaffold (CGP),[23b, 24] in this work we describe a series of tailored ditopic molecular modules that, through the formation of EBIs and XBIs, crystallized into solids through the formation of programmed heteromolecular supramolecular polymers.

Design of multi-component supramolecular polymers. In our crystal-engineering approach, the idea is to prepare supramolecular polymers at the solid state through a co-crystallisation of two ditopic molecular modules: the chalcogen (Ch) and halogen (Hal) modules, respectively (Scheme 1). While

the Ch modules are heterotopic, *i.e.* bearing two diverse recognition groups, the Hal synthons are homotopic. The Ch modules are supposed to undergo self-association through double EBIs as established through the CGP-based recognition units, whereas the Hal building blocks should interact with the Ch counterpart through XBIs.
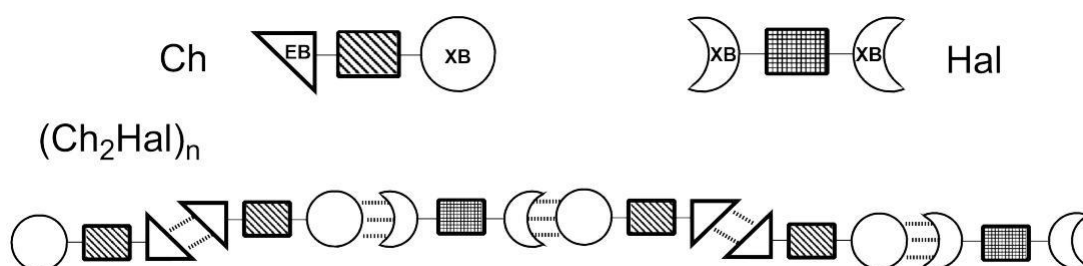
Scheme 1. Schematic representation of the molecular modules Ch and Hal and of the general structure of the supramolecular polymer at the solid state.

Depending on the role taken in the formation of the interaction and the nature of the functional group on the Ch synthon, the Hal module can act either as XB-donor or EB-acceptor.[25] Supramolecular polymers at the solid state with a repetition unit of $(Ch_2Hal)_n$ are expected to form upon evaporation of a solution containing a mixture of both Ch and Hal components. The designed supramolecular Ch and Hal synthons are depicted in Scheme 2. While CGP-based molecules 1^E and 2^E feature a XB-acceptor pyridyl-type substituent, modules 4^E and 5^E expose at 2-position bromo- and iodo-tetrafluorophenyl moieties. Both Se-and Te-congeners were synthesized following the protocols previously reported by us (see SI for the synthesis).[16a, 27] As

far as the ditopic Hal synthons are concerned, hexadecafluoro-1,8-diiodooctane (**HDFIO**) and 1,4-diiodo-2,3,5,6-tetrafluorobenzene (**DITFB**) were chosen as XB donors, and 4,4'-bipyridyl (**biPy**) and 1,4-diazabicyclo[2.2.2]octane (**DABCO**) as XB acceptors.[25] These modules are well-known building blocks used to trigger XBIs at the solid state.[25]
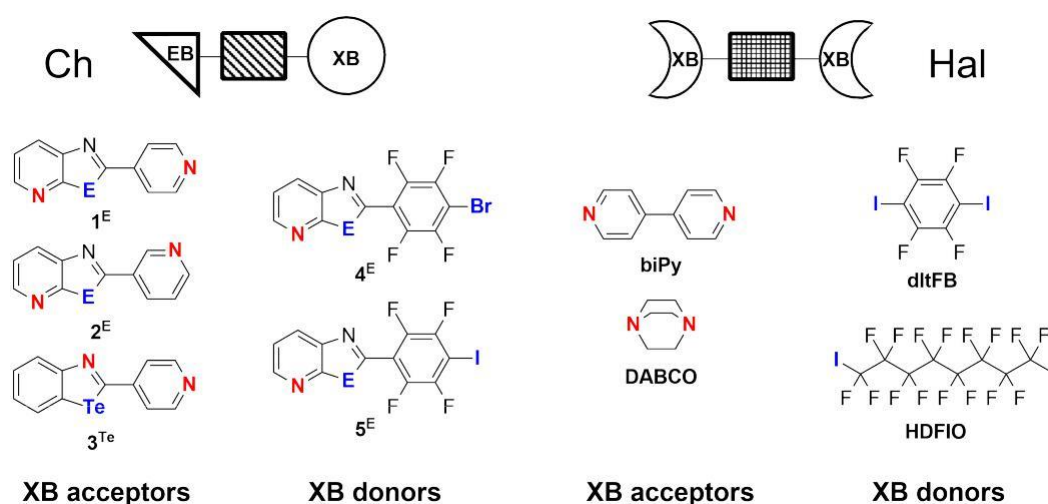
Scheme 2. Chemical structure of the self-assembly ditopic synthons.

At last, reference benzochalcogenazole **3Te**[16e,26] was also prepared and studied in combinations with the appropriate XB donor. It is expected that molecule **3Te** forms wire-like structures through Te$^{...}$N$_C$ interactions,[16e] and lateral XB contacts engaging the pyridyl moiety with the ditopic XB acceptor (Hal). The anticipated repeating units of the devised supramolecular polymers are reported in Schemes 3 and 4.

6
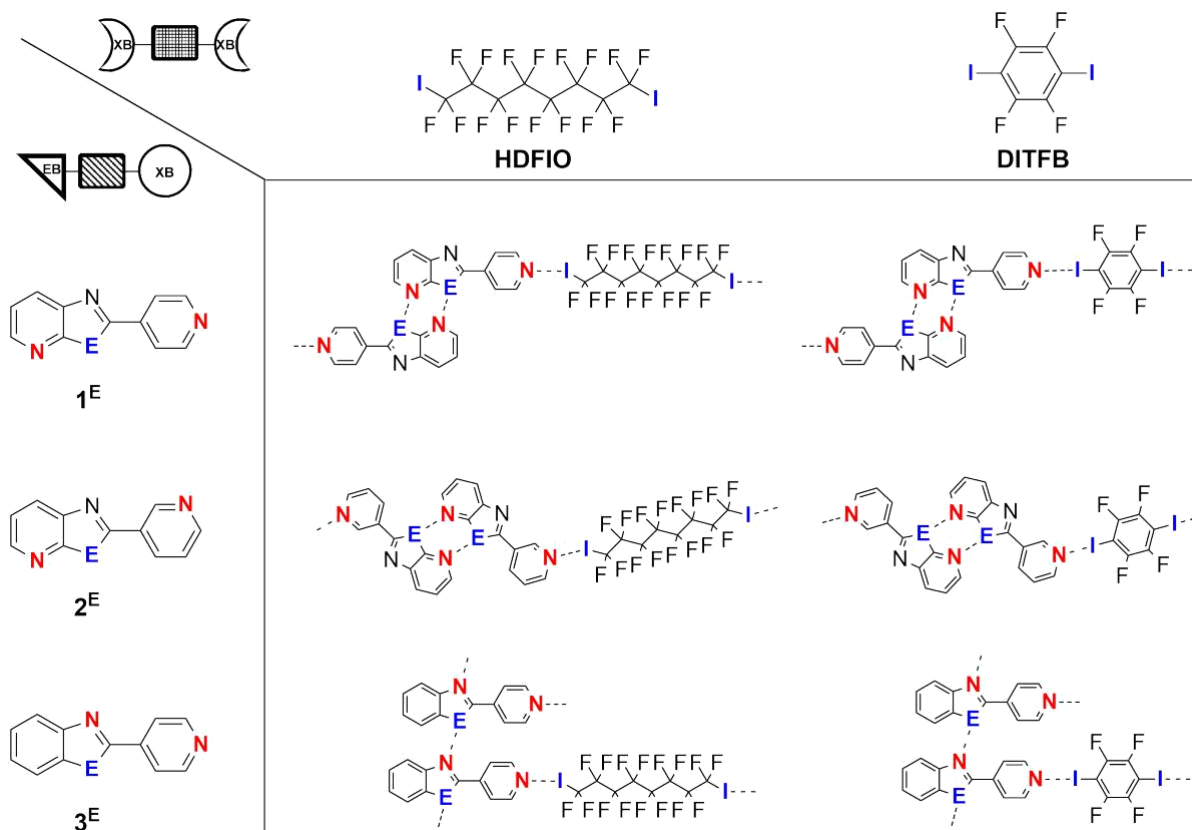
Scheme 3. Envisaged supramolecular polymers deriving from the combinations of molecules **1E**, **2E** and **3E** with either **HDFIO** or **DITFB** XB-donor synthons.

Te-analogues **1Te** and **2Te** are expected to engage in frontal double EBIs leading to dimers, which could successively express XB contacts with either **HDFIO** or **DITFB** (Scheme 3). Likewise, molecules **4E** and **5E** (Scheme 4) are expected to dimerise though double EBIs and undergo polymerisation in the presence of **biPy** and **DABCO** through XBIs with Br/I atoms. To validate the recognition abilities of the designed self-assembling synthons, we used electrostatic surface potential (ESP)[16e, 23b, 27] and estimated the value ($V_{s,max}$) at the point of the highest charge for both donor and acceptor atoms at B97D3/Def2-TZVP level of

theory using Gaussian09 including D01 revision.[16e, 23b, 27] The

ESPs of all molecular modules are shown in Table 1.
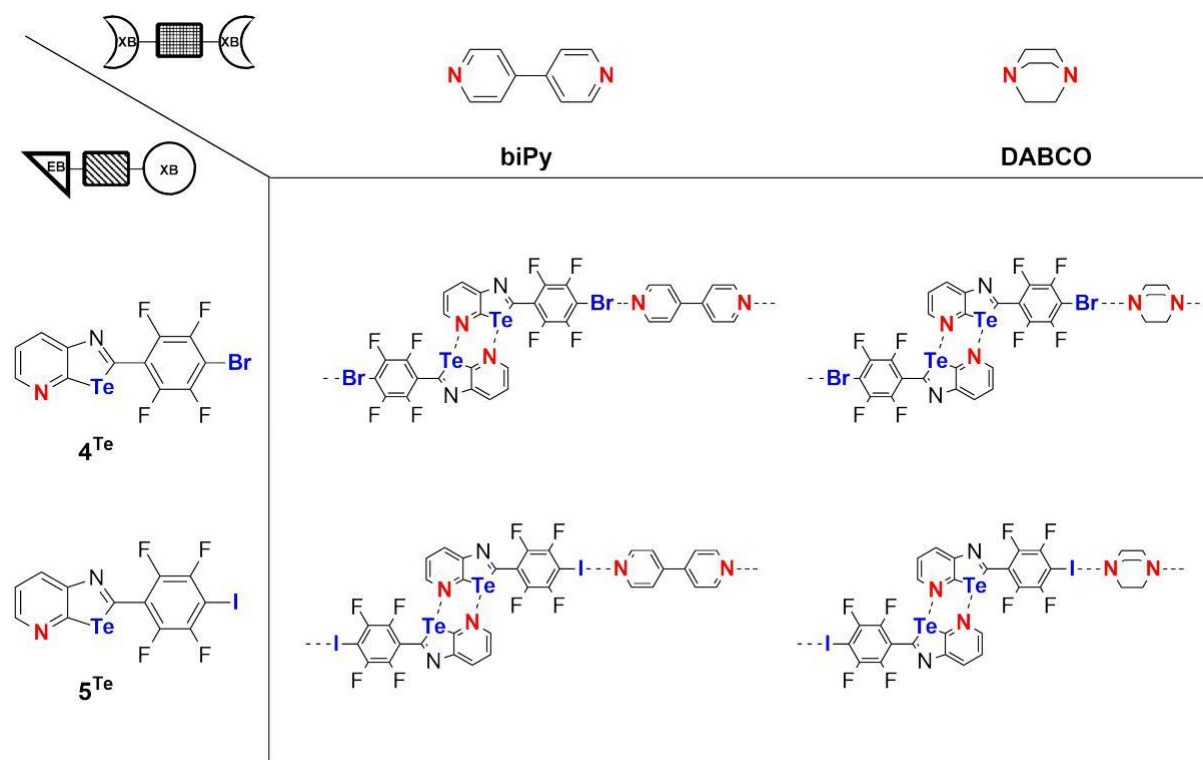
Scheme 4. Envisaged supramolecular polymers deriving from the combinations of molecules **4^Te** and **5^Te** with either **biPy** or **DABCO** XB-acceptor synthons.

The images highlight positive potential regions (blue) around Te,

Se, Br and I atoms and electron donor as negative potential

region (red) around N atoms. The surface around the halogens and

chalcogen atoms are clearly distributed in two parts: the *S*-hole

(in blue) and the negative belt (yellow-green). As expected, the

S-holes are deeper for Te and I than for Se and Br atoms.

Table 1. Calculated ESP and $V_{s,max}$ values (kcal mol^{-1}). N_p = N of pyridyl ring, N_c = N of chalcogenazole ring, X = N, Br, I (heteroatoms engaging in XBIs).

Module	ESP maps		$V_{s,max}$ (kcal mol^{-1})			
	Top view	Side view	N_p	N_c	X	σ-hole (α)
1^{Se}			−26.8	−15.1	−33.0	+7.09
1Te			−26.1	−13.9	−32.9	+12.5
2^{Se}			−28.8	−15.7	−31.4	+5.02
2Te			−27.0	−14.4	−31.0	+10.7
3Te			−	−16.9	−33.9	+23.5
4Te			−25.3	−21.3	+22.2	+12.9
5Te			−27.3	−13.9	+30.4	+12.5
HDFIO			−	−	+27.6	−
DITFB			−	−	+29.5	−
biPy			−	−	−32.0	−
DABCO			−	−	31.0	−
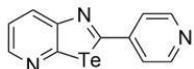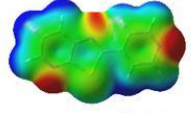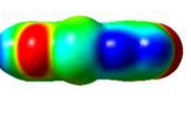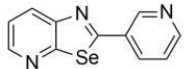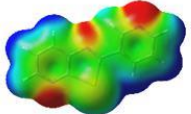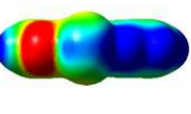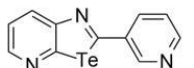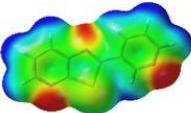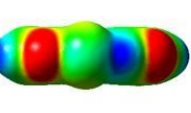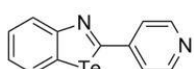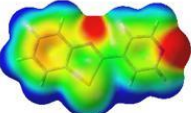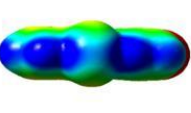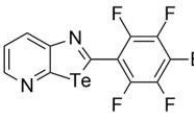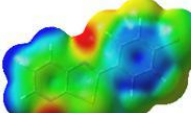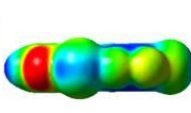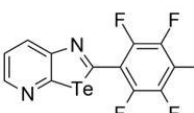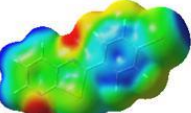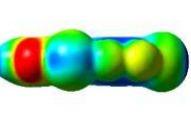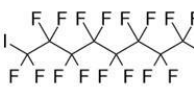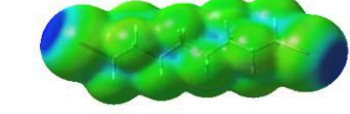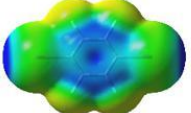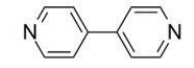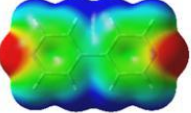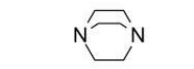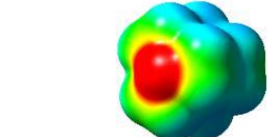
-0.025 a.u.   +0.025 a.u.

For the sake of this work, we will focus only on the σ-hole(a) as the σ-hole(b) do not intervein in the formation of the EBIs in these systems (the σ-hole(a) and σ-hole(b) for describing positive electrostatic regions on the chalcogen atom exposed on the side of the 4- and 2-positions, respectively, as proposed previously by us).[16e] The formation of the supramolecular polymers is discussed considering ESPs (Table 1). As already suggested previously,[16e, 23b] the σ-hole displaying the highest positive $V_{s,max}$ value will engage in the SBI with the functional group featuring the most electronegative heteroatom (*i.e.*, the most negative $V_{s,max}$ value).[16e, 23b]

Results and discussion

Co-crystal preparation. All co-crystallization attempts are summarized in Table 2. Solutions of the given components in a stoichiometry of choice were prepared in $CHCl_3$ and left standing for slow evaporation. The nomenclature of each co-crystals is given by the minimal repetition unit of the supramolecular structure formed at the solid state, whereas the supramolecular species (oligomers and polymers) triggered by the chalcogen- and halogen-bonding in the co-crystal are labelled as polymeric structures (Table 2). Molecule **1Te** forms co-crystals 2:1 with both **HDFIO** and **DITFB**, mirroring the solution stoichiometry (entries 1 and 2). Co-crystals with 1:1 and 1:2 stoichiometries containing supramolecular polymer **(1Te•DITFB)$_n$** and aggregate **(1Te•(DITFB)$_2$)$_n$** could be obtained with **DITFB** when starting from

solutions of 1:1 and 1:10 ratios, respectively (entries 3 and 4).

Table 2. Co-crystallization attempts, stoichiometries in solution (o:p)^{sol} and in the resulting co-crystals (o:p)^{coc} (with the o and p standing for the Ch and Hal components, respectively). Solvent: $CHCl_3$. *Crystal segregation.

Entry	Ch	Hal	(o:p)^{sol}	(o:p)^{coc}	Co-crystal	Supramolecular entity
1	1^{Te}	HDFIO	2:1	2:1	$1^{Te}_2 \bullet$HDFIO	$(1^{Te}_2 \bullet HDFIO)_n$
2	1^{Te}	DITFB	2:1	2:1	$1^{Te}_2 \bullet$DITFB	$(1^{Te}_2 \bullet DITFB)_2$
3	1^{Te}	DITFB	1:1	1:1	$1^{Te} \bullet$(DITFB)$_n$	$(1^{Te} \bullet DITFB)_n$
4	1^{Te}	DITFB	1:10	1:2	$1^{Te} \bullet$(DITFB)$_2$	$(1^{Te} \bullet (DITFB)_2)_n$
5	2^{Te}	HDFIO	2:1	–*	–	–
6	2^{Te}	DITFB	2:1	2:1	$2^{Te}_2 \bullet$DITFB	$(2^{Te}_2 \bullet DITFB)_n$
7	2^{Te}	DITFB	1:1	2:1	$2^{Te}_2 \bullet$DITFB	$(2^{Te}_2 \bullet DITFB)_n$
8	2^{Te}	DITFB	1:3	2:1	$2^{Te}_2 \bullet$DITFB	$(2^{Te}_2 \bullet DITFB)_n$
9	3^{Te}	HDFIO	2:1	2:1	$3^{Te}_2 \bullet$HDFIO	$3^{Te}_2 \bullet HDFIO$
10	3^{Te}	DITFB	2:1	2:1	$3^{Te}_2 \bullet$DITFB	$3^{Te}_2 \bullet DITFB$
11	1^{Se}	HDFIO	2:1	–*	–	–
12	1^{Se}	DITFB	2:1	2:1	$1^{Se}_2 \bullet$DITFB	$(1^{Se}_2 \bullet DITFB)_2$
13	1^{Se}	DITFB	1:1	2:1	$1^{Se}_2 \bullet$DITFB	$(1^{Se}_2 \bullet DITFB)_2$
14	1^{Se}	DITFB	1:10	1:2	$1^{Se} \bullet$(DITFB)$_2$	$(1^{Se} \bullet (DITFB)_2)_n$
15	2^{Se}	DITFB	2:1	2:1	$2^{Se}_2 \bullet$DITFB	$(2^{Se}_2 \bullet DITFB)_n$
16	4^{Te}	biPy	2:1	–*	–	–
17	4^{Te}	DABCO	2:1/10:1	–*	–	–
18	5^{Te}	biPy	2:1/10:1	–*	–	–
19	5^{Te}	DABCO	1:2	–*	–	–
20	5^{Te}	DABCO	1:5	2:1	$5^{Te}_2 \bullet$DABCO	$(5^{Te}_2 \bullet DABCO)_n$
21	5^{Te}	DABCO	1:10	1:1	$5^{Te} \bullet$DABCO	$(5^{Te} \bullet DABCO)_2$
22	1^{Te}	5	1:1	1:1	$1^{Te} \bullet 5^{Te}$	$(1^{Te} \bullet 5^{Te})_n$

Crystal segregation was observed when isomer 2^{Te} was co-crystallized with **HDFIO** (entry 5), whereas polymer $(2^{Te}_2 \cdot DITFB)_n$ crashed out from the solution with **DITFB** independently on the solution stoichiometry (entries 6-8). Notably, reference molecule 3^{Te} forms co-crystals with 2:1 stoichiometry with both XB donors (entries 9 and 10, respectively). Evaporation of a solution of Se-analogue 1^{Se} with **HDFIO** did not give rise to any co-crystals (entry 11), whereas solutions containing 2:1 and 1:1 ratio of **DITFB** (entries 12 and 13) exclusively gave co-crystals with stoichiometry of 2:1, with the molecules aggregated as supramolecular hexamers $(1^{Se}_2 \cdot DITFB)_2$. Notably, when using an excess of **DITFB** (1:10), co-crystals of aggregate $(1^{Se} \cdot (DITFB)_2)_n$ were formed (entry 14), as observed with the Te-analogue. Moving to the pyrid-3-yl isomer (2^{Se}), co-crystals of stoichiometry 2:1 were obtained as large yellow plates, also containing a polymer-like organization (entry 15). When we reversed the XB demand, co-crystallization experiments with compound 4^{Te} in the presence of **biPy** and **DABCO** were unsuccessful (entries 16 and 17, respectively) and crystal segregation was observed. Similar results were obtained with iodo-derivative 5^{Te} with both **biPy** and **DABCO**. However, when using an excess of **DABCO**, co-crystals with 2:1 and 1:1 stoichiometries were obtained as large yellow prisms (entries 20 and 21, respectively). While the 2:1 solid contains supramolecular polymer $(5^{Te}_2 \cdot DABCO)_n$,cin the 1:1 co-crystal the molecules are arranged as tetrameric species, $(5^{Te} \cdot DABCO)_2$. Finally, when mixing XB acceptor 1^{Te} and XB donor 5^{Te} in a 1:1

ratio in CHCl$_3$, co-crystals 1:1 containing polymer (**1Te•5Te)$_n$** were obtained (entry 22).

Solid-state supramolecular polymers with Te-CGP bearing halogen-bond acceptors. X-ray diffraction analysis of co-crystals **1$^{Te}_2$•HDFIO** reveals the formation of supramolecular polymer **(1$^{Te}_2$•HDFIO)$_n$** through a 2:1 association (Fig. 1).
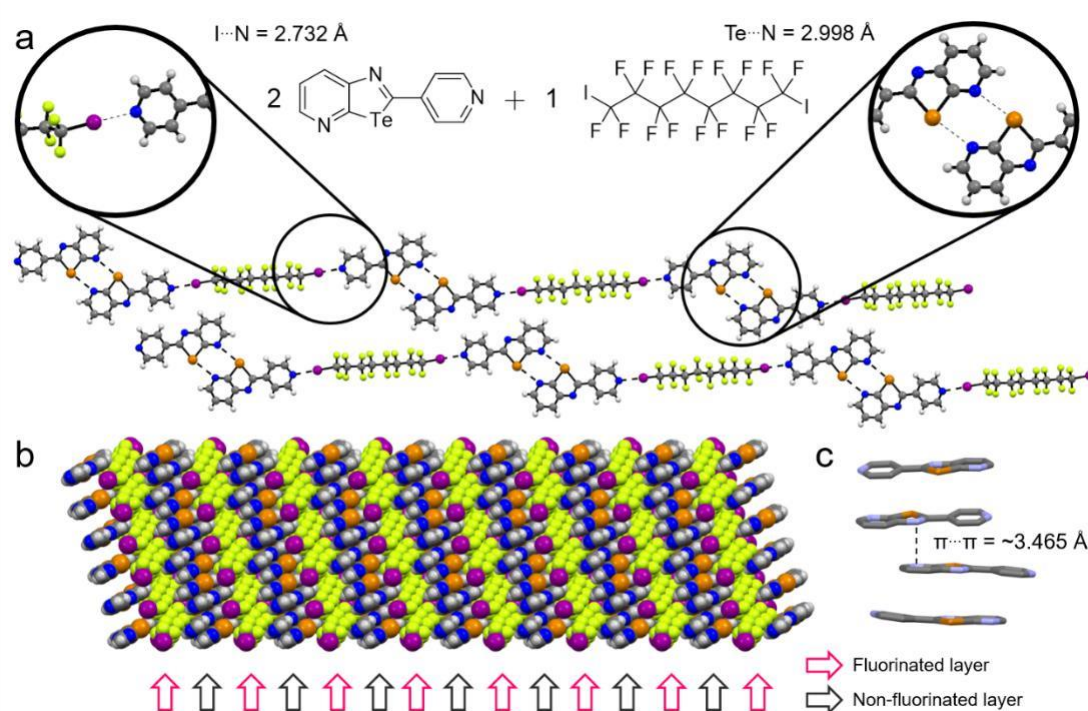
Figure 1. X-ray structure of co-crystal **1$^{Te}_2$•HDFIO** a) evidencing the formation of polymer **(1$^{Te}_2$•HDFIO)$_n$**; b) vdW sphere representation of the layered organization; c) p-p stacking arrangement. Space group: P$\bar{}$. Atom colors: blue N, ocher Te, yellow F, pink I, gray C.

One can easily discern the dimeric association of the CGP motif through double EBIs (d$_{N...Te}$ = 2.998 Å). Each pair of **1Te** sandwiches a molecule of **HDFIO** through two XB contacts established with the pyrid-4-yl moieties (d$_{N...I}$ = 2.732 Å). Notably,

tellurazolopyridine 1^{Te} arranges in columnar p-p stacks (estimated d_{p-p} = 3.465 Å) in a head-to-tail arrangement (Fig. 1c) separated by a layer of **HDFIO**. The solid-state arrangement led to a segregation between the fluorinated (pink arrows) and non-fluorinated (grey arrows) moieties (Fig. 1b). Replacing **HDFIO** with **DITFB** (Fig. 2) led to polymer **$(1^{Te}{}_2•DITFB)_n$**.
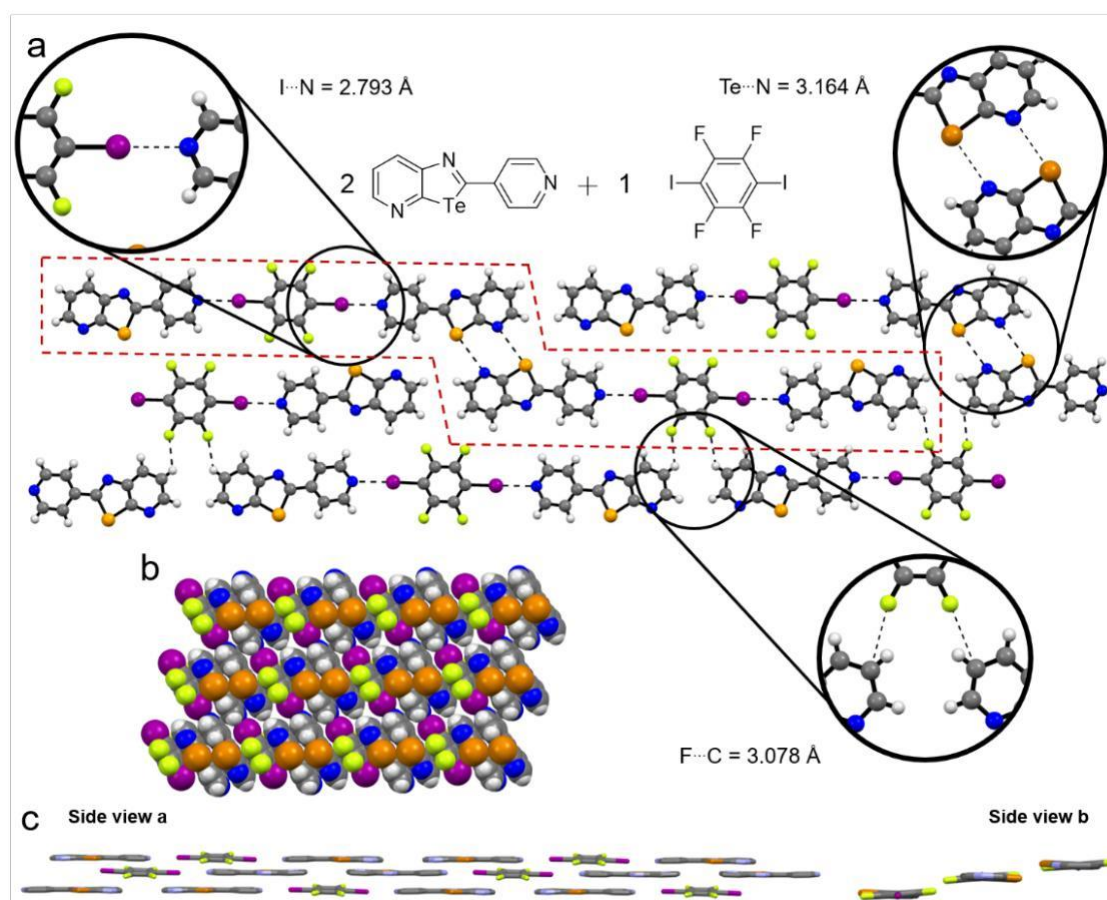
Figure 2. X-ray structure of co-crystal **$1^{Te}{}_2•DITFB$**, forming a) hexameric units **$(1^{Te}{}_2•DITFB)_2$**; b) vdW sphere representation of the layered organization; c) off-set arrangement. Space group: P". Atom colors: blue N, ocher Te, yellow F, pink I, gray C.

In this case, the synthons arrange in hexameric structures (contoured with a red dashed line), where the two central CGP

moieties liaise through double EBIs ($d_{N...Te}$ = 3.164 Å) and DITFB

is sandwiched between two pyrid-4-yl moieties ($d_{N...I}$ = 2.793 Å).

Each hexamer is brought together by weak HB interactions engaging

the H-atom in 6-position of the terminal CGP group and two F

atoms from DITFB ($d_{F...H-C}$ = 3.078 Å). Those interactions organize

the hexamer in a quasi-planar arrangement (off-set between two

overlapping layers: 0.912 Å, Fig. 2c). In addition, DITFB

interacts with two CGP units through quasi-parallel p-p stacking

interactions (Fig. 2c). Molecule 1^{Te} arranges in a head-to-tail

fashion (estimated d_{p-p} = 3.490 Å) and the fluorinated aromatic is

sandwiched between two tellurazolopyridines (d_{p-p} = 3.580 Å).
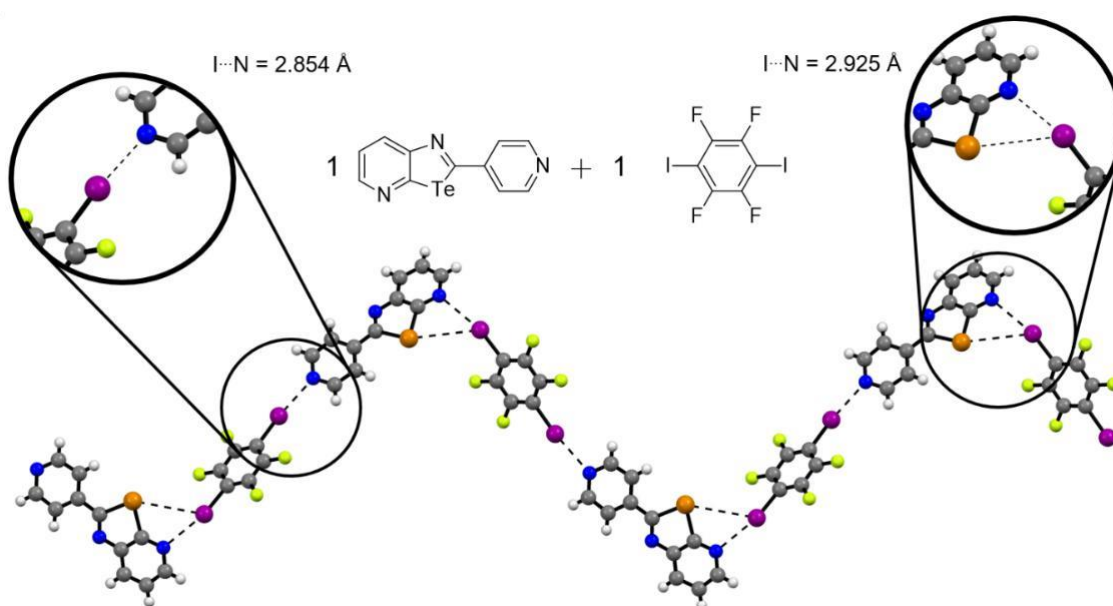
Figure 3. X-ray structure of co-crystal 1^{Te}•DITFB evidencing only the formation of XBIs. Space group: P2$_1$/n. Atom colors: blue N, ocher Te, yellow F, pink I, gray C.

Looking at the ESP map (Fig. S18), one can observe that the

p-surfaces of **DITFB** and **CGP** feature opposite potentials. This

complementary quadrupolar charge distribution is likely to

govern the face-to-face arrangement at the solid state. In analogy to the 1:1 case (**1Te•DITFB**, Fig. 3), the 1:2 co-crystals (**1Te•(DITFB)$_2$**, Fig. 4) does not show any noticeable double EBIs between the CGP moieties. Rather, only XBIs and HBIs are present (Fig. 4). Specifically, **DITFB** interacts through XB contacts with the pyrid-4-yl (d$_{N...I}$ 2.804 Å) and the CGP (d$_{N...I}$ = 2.754) groups.
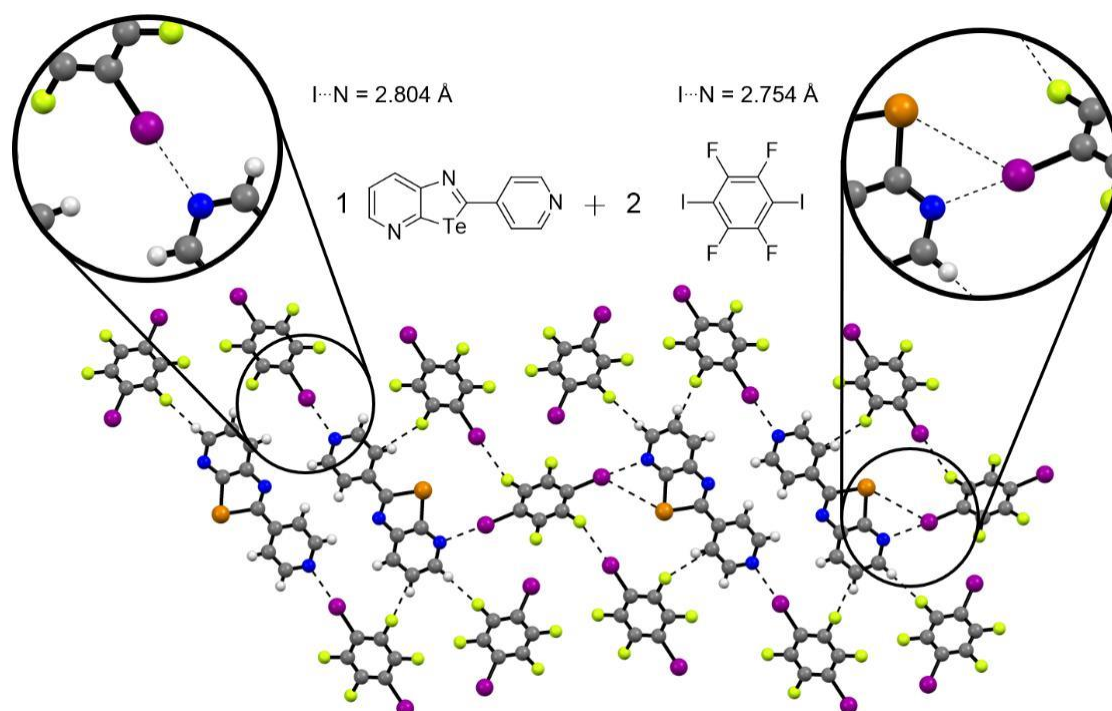
Figure 4. X-ray structure of **1Te•(DITFB)$_2$** evidencing only the formation of XBIs. Space group: P . Atom colors: blue N, ocher Te, green F, pink I, gray C.

When compared to the solid-state arrangement of **1Te•DITFB** (Fig. 3), the XBI established with the CGP moiety is shorter than that formed with the pyrid-4-yl moieties. As observed in the co-crystals of **1Te•DITFB**, the I and Te atoms interact through weak EBIs (d$_{I...Te}$ = 4.005 Å, S$_{vdW}$ = 4.04 Å), with the former atom acting

as the chalcogen-bond donor and the latter as the chalcogen-bond acceptor (Fig. 3).

When moving to the co-crystals of molecules 2^{Te} and **DITFB**, supramolecular polymer $(2^{Te}_2 \cdot DITFB)_n$ was formed independently on the stoichiometry (Table 2, Fig. 5). The structure displays the CGP group engaging into double EBIs ($d_{N...Te}$ = 3.068 Å), and the two pyrid-3-yl moieties forming XBIs ($d_{N...I}$ = 2.738 Å) with **DITFB**.

Both 2^{Te} and **DITFB** homomolecularly p-p stack (d_{p-p} = 3.544 Å and 3.459 Å, off-set of 2.945 Å and 3.339 Å, Fig. S20).
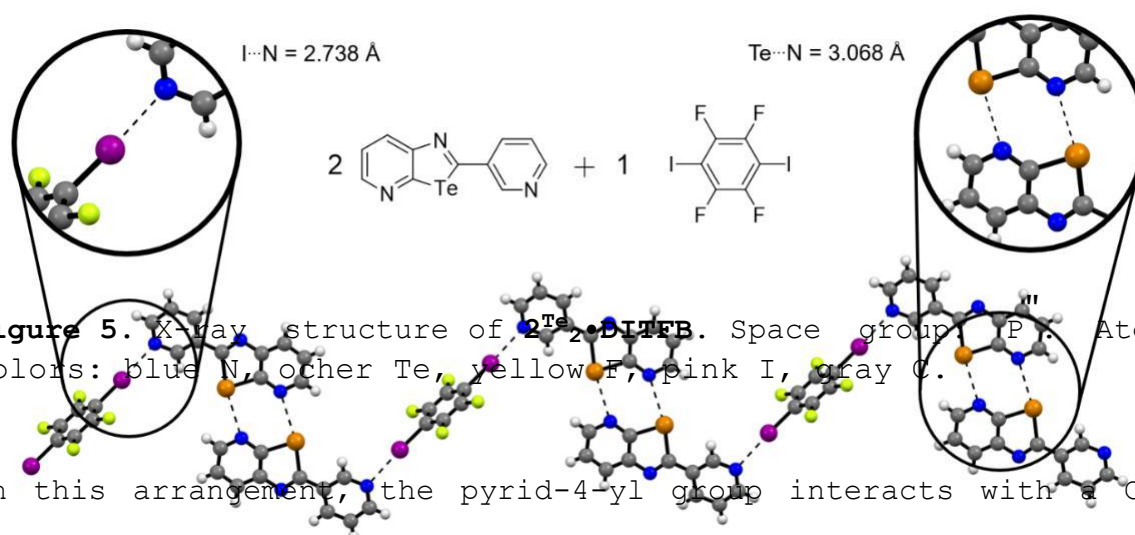
Figure 5. X-ray structure of $2^{Te}_2 \cdot DITFB$. Space group P . Atom colors: blue N, ocher Te, yellow F, pink I, gray C.

In this arrangement, the pyrid-4-yl group interacts with a CGP moiety through a double hetero non-covalent interaction, namely frontal EBI ($d_{N...Te}$ = 3.000 Å) and HBI ($d_{N...C}$ = 3.568 Å). The CGP group of the inverted arrangement interacts through an XBI with **DITFB** ($d_{N...I}$ = 2.984 Å). At the molecular level, one can easily notice that the ESP is rather symmetrical (Fig. 6b), suggesting

that both electrostatic arrangements are possible without significantly disrupting the crystal organisation (Fig. 6c).
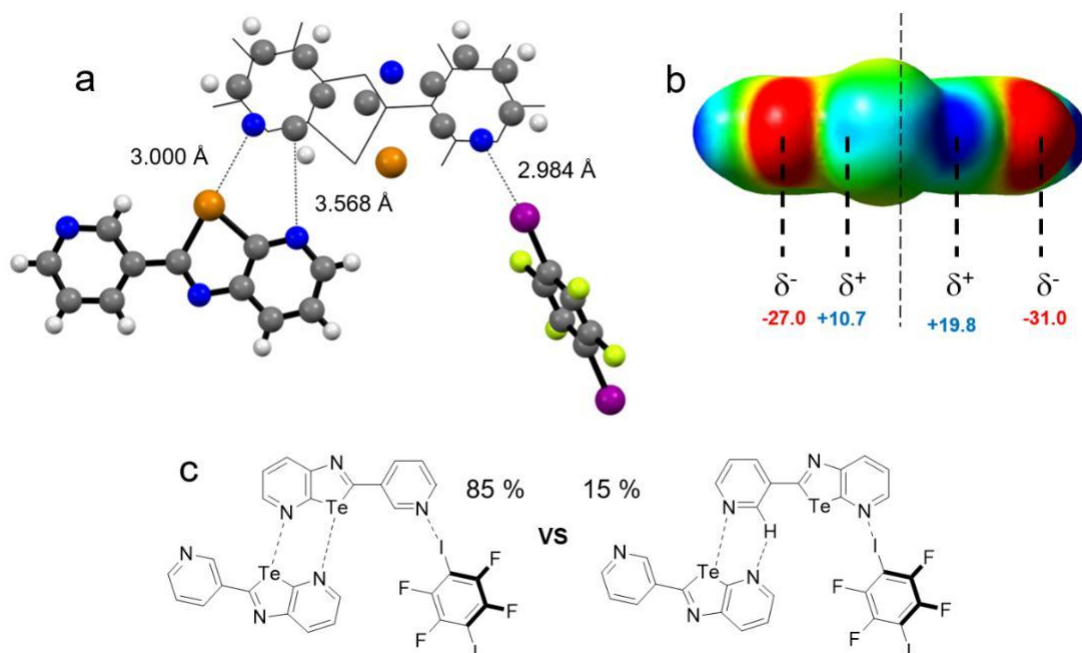
Figure 6. The two arrangement modes a) and c) for molecule **2Te** in **2$^{Te}_2$•DITFB**. b) ESP map for **2Te**, level of theory: B97D3/Def2-TZVP using Gaussian09 including D01 revision. Atom colors: blue N, ocher Te, yellow F, pink I, gray C.

Moving to reference molecule **3Te**, co-crystals with 2:1 stoichiometry, **3$^{Te}_2$•HDFIO** (Fig. 7) and **3$^{Te}_2$•DITFB** (Fig. 8), were obtained with both molecules **HDFIO** and **DITFB**, respectively. As far as **3$^{Te}_2$•HDFIO** is concerned, no EBIs have been observed. Only XBIs between pyrid-4-yl moieties and **HDFIO** were present ($d_{N...I}$ = 2.772 Å and 2.819 Å, Fig. 7). As in the case of **1$^{Te}_2$•HDFIO**, a segregation of the fluorinated (indicated by pink arrows) and non-fluorinated (indicated by grey arrows) synthons is observed.
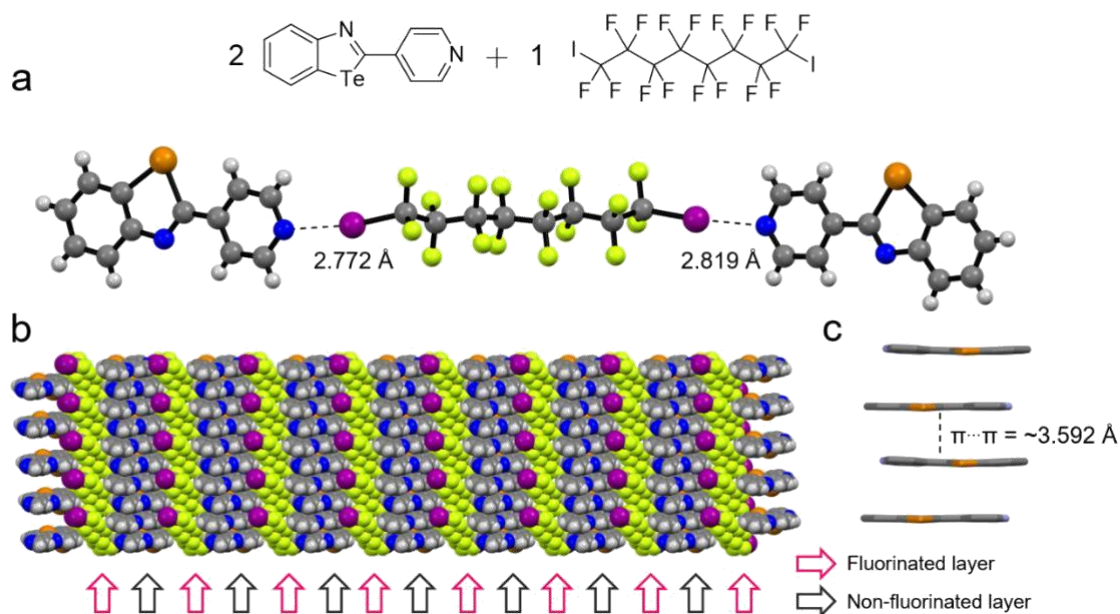
Figure 7. X-ray structure of co-crystal **3$^{Te}_2$•HDFIO** displaying the
a) structure of repetitive unit **3$^{Te}_2$•HDFIO**; b) vdW sphere representation of the layered organization; c) p-p stacking arrangement. Space group: P". Atom colors: blue N, ocher Te, yellow F, pink I, gray C.

The X-ray diffraction analysis of co-crystal **3$^{Te}_2$•DITFB** (Fig. 8) shows the presence of trimeric units in which the XB donor is sandwiched between two pyrid-4-yl moieties through XBIs ($d_{N...I}$ = 2.823 Å). Moreover, the tellurazole unit engages in an EBI with one of the F atoms of **DITFB** ($d_{F...Te}$ = 3.294 Å). Similarly to **1$^{Te}_2$•DITFB**, quasi-parallel p-p stacks are formed, alternating one **DITFB** module and two molecules of **3Te** (estimated d_{p-p} = 3.370 Å between **DITFB** and **3Te**, d_{p-p} = 3.690 Å between two **3Te**), the latter being arranged in a head-to-tail fashion (Fig. 8b-c). Taken all together, the studies with reference molecule **3Te** suggested that synthons forming only single EBIs are not ideal candidates for engineering co-crystals with concurring XBIs.

19
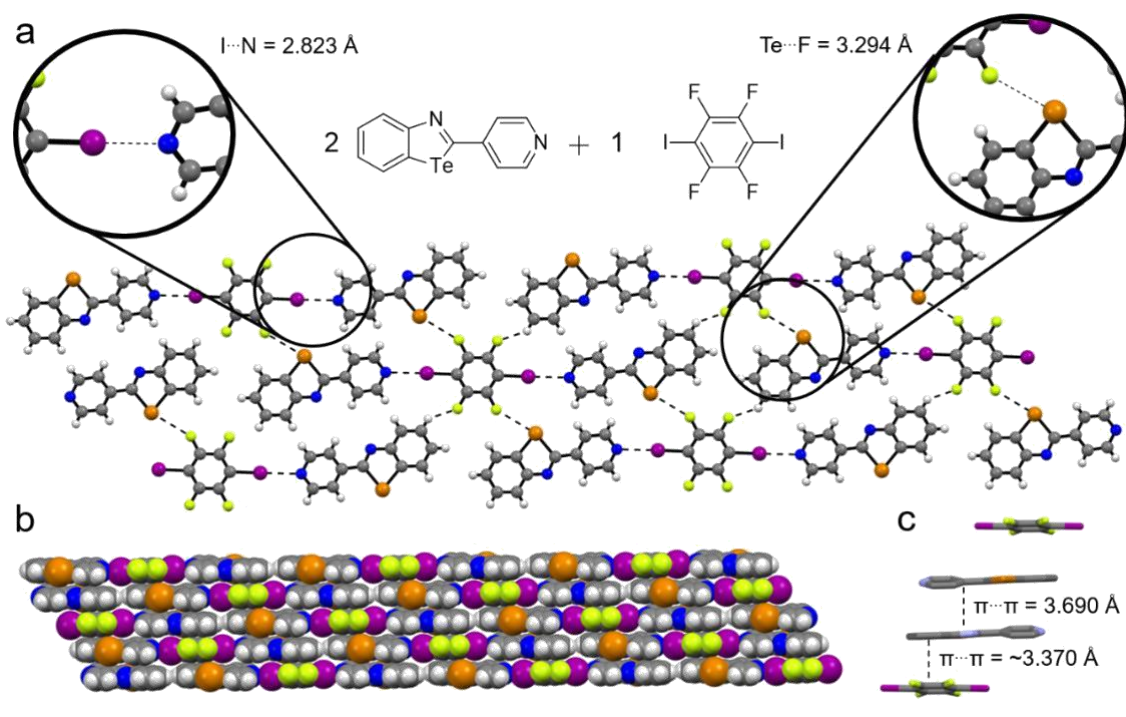
Figure 8. a) X-ray structure of 2:1 co-crystal **3$^{Te}_2$•DITFB**; b) vdW sphere representation; c) p-p stacking arrangement. Space group: P". Atom colors: blue N, ocher Te, yellow F, pink I, gray C.

Solid-state supramolecular polymers with Se-CGP bearing halogen-bond acceptors. To study the effect of the chalcogen atom donor, we also have grown co-crystals between the Se-doped CGP derivatives (**1^{Se}** and **2^{Se})** and the halogen-donor modules (Table 2). X-ray analysis of **1$^{Se}_2$•DITFB** (Fig. 9) reveals that the molecules associate in hexameric structures **(1$^{Se}_2$•DITFB)$_2$**, as observed for **1$^{Te}_2$•DITFB** (Fig. 1). In the hexamer, the two central CGP groups interact through frontal dual EBIs ($d_{N...Se}$ = 3.294 Å) while establishing lateral XB contacts with **DITFB** ($d_{N...I}$ = 2.779 Å). In the crystal packing, the hexamers are connected through weak HBIs between the hydrogen atom in the 6-position of terminal CGP moieties and the F atoms ($d_{F...C}$ = 3.088 Å). This forces all

20

modules to adopt a quasi-planar arrangement, displaying a minor misalignment of 0.976 Å (Fig. 9c). These observations contrast previous results in the group, for which the X-ray structure of crystals containing only 1^{Se} did not show any EBIs dimerization.
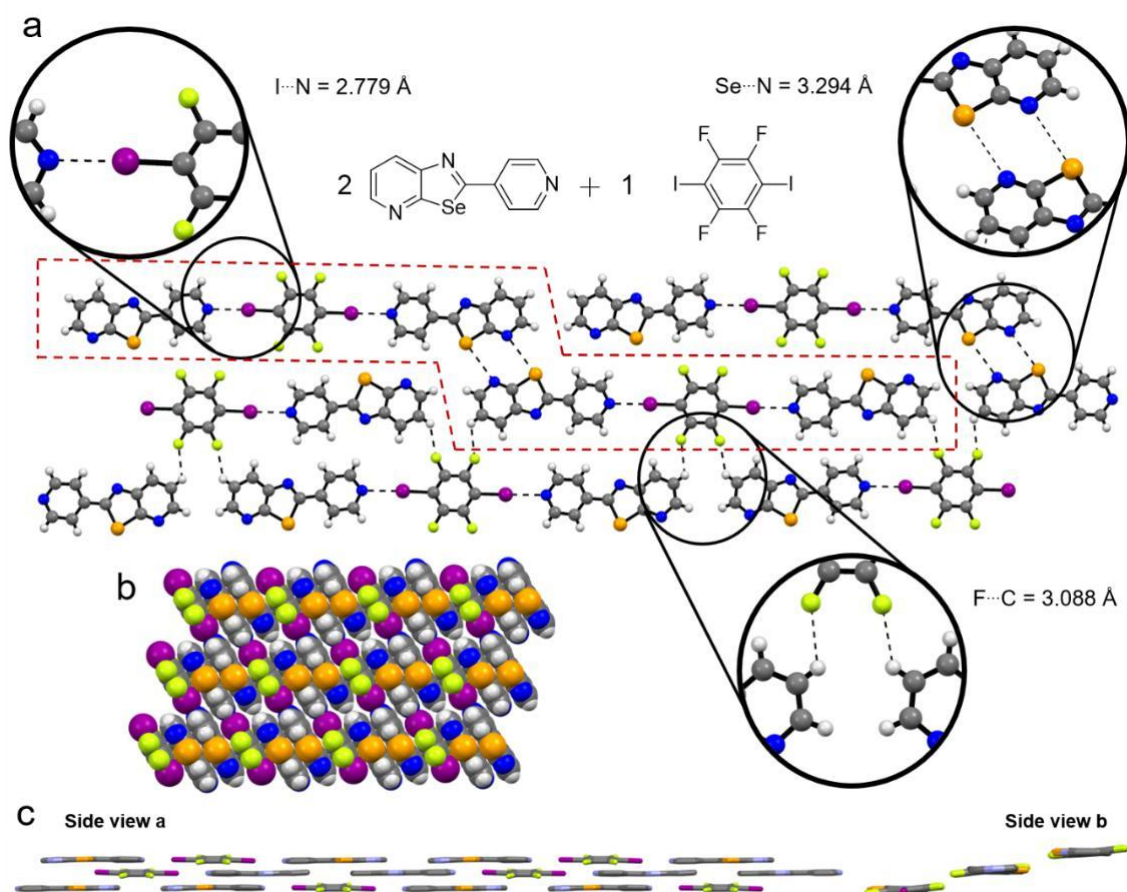
Figure 9. X-ray structure of co-crystal $1^{Se}_2 \cdot DITFB$. a) Supramolecular polymer; b) vdW sphere representation; c) capped stick representation of the miss-alignment. Space group: P". Atom colors: blue N, ocher Te, yellow F, pink I, gray C.

However, when looking at ESP map of $1^{Se} \cdot DITFB$ (Fig. 10), one can notice $V_{s,max}$ value of the Se-centered s(a) has increased to +11.3 kcal mol^{-1} upon interaction with **DITFB** from the value of +7.09 kcal mol^{-1} for molecule 1^{Se} alone. This suggests that once a pyrid-4-yl moiety contacts a **DITFB**, it seemingly depletes the Se-CGP

21

moiety, raising the strength of the double EBIs. This observation is accordance with previous results, for which CF3-bearing Se-CGP derivatives form doubly EB-bonded dimers.[26b]
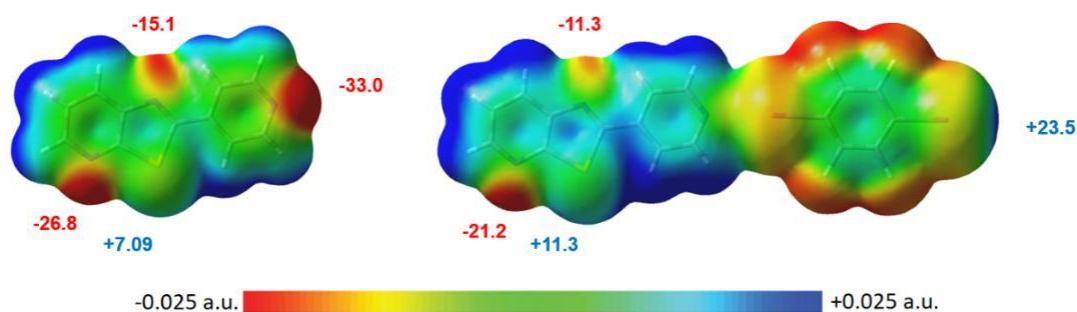
Figure 10. ESP map of **1^Se** (left) and of a **1^Se•DITFB** complex held by a XBI (right) . Extreme values of interest are highlighted. Level of theory: B97D3/Def2-TZVP using Gaussian09 including D01 revision.
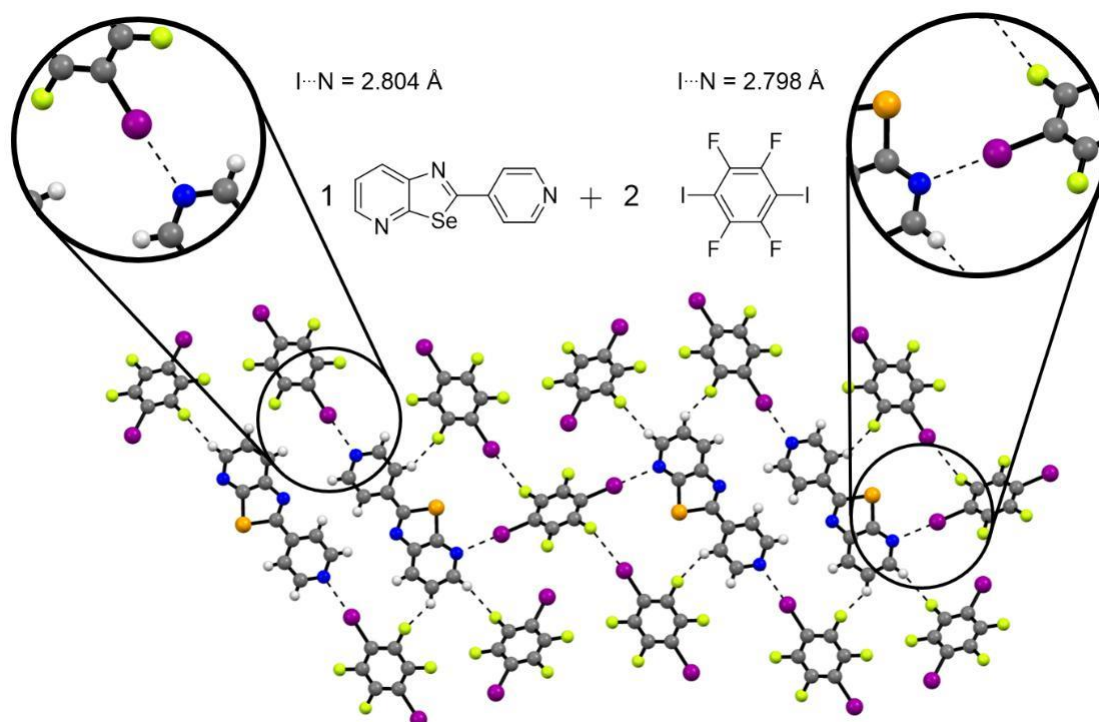
Figure 11. X-ray structure of 1:2 co-crystal **1^Se•(DITFB)₂** evidencing the key SBIs. Space group: P". Atom colors: blue N, ocher Te, yellow F, pink I, gray C.

Co-crystal **1^{Se}•(DITFB)$_2$** is iso-structural to **1Te•(DITFB)$_2$**. The pyrid-4-yl groups and the CGP moieties interact with two crystallographically independent molecules of **DITFB** through XB contacts (d$_{N...I}$ 2.804 Å and d$_{N...I}$ = 2.798 Å, respectively, Fig. 11). In contrast to the case of **1Te•(DITFB)$_2$**, no XBs are observed between Se and I atoms. Crystallization experiments using isomer **2^{Se}** led to co-crystal **2^{Se}$_2$•DITFB** (Fig. 12).
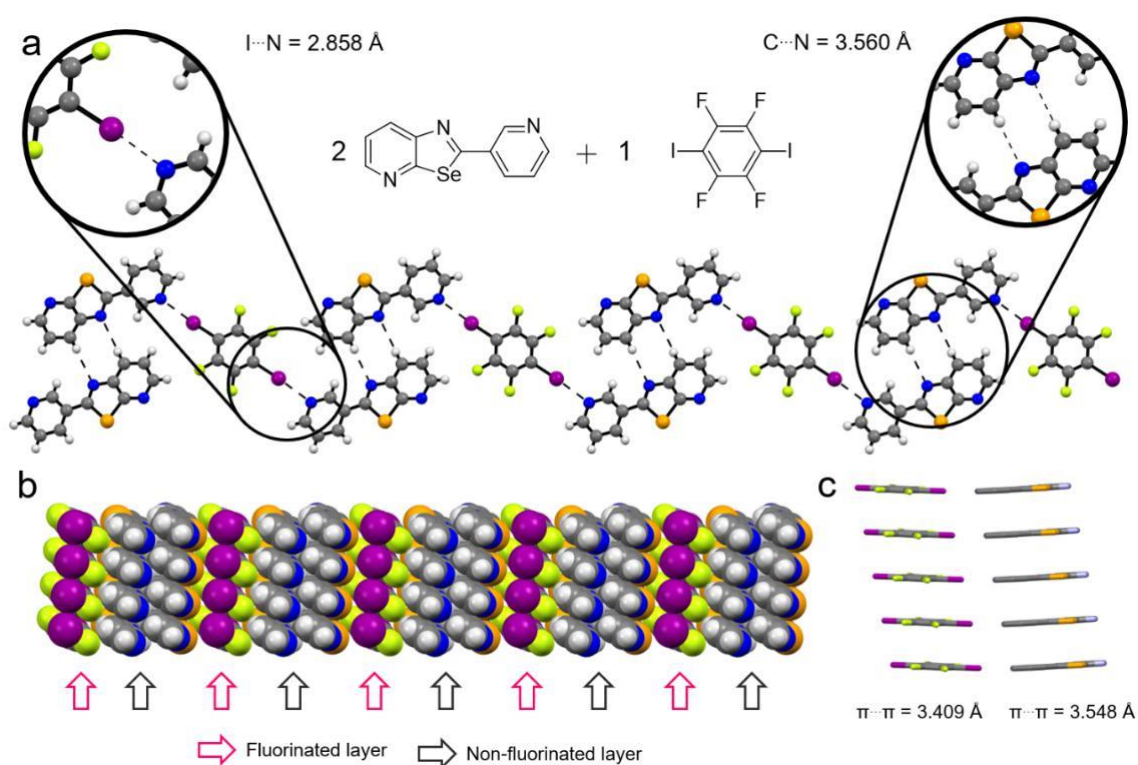
Figure 12. X-ray structure of co-crystal **2^{Se}$_2$•DITFB**. a) Supramolecular polymer; b) vdW sphere representation of the layered organization; c) capped stick representation of the p-p stacking. Space group: P$\overline{1}$. Atom colors: blue N, ocher Te, yellow F, pink I, gray C.

In the structure, the Se-derivative associate in dimers through HB interactions (d$_{N...C}$ = 3.560 Å) and develop into a supramolecular polymer through XB contacts with the I atom (d$_{N...I}$

= 2.858 Å). This results in a quasi-co-planar organization of the molecules. In addition, **2$^{\text{Se}}$** and **DITFB** interact through p-p stacking (p-p = 3.548 Å and 3.409 Å, with an off-set of 1.843 Å and 2.089 Å, respectively) piling into columns of fluorinated (indicated by pink arrows) and non-fluorinated (indicated by grey arrows) domains (Fig. 12b-c). Surprisingly, the co-crystals do not feature any EBIs, in contrast to the case of **1$^{\text{Se}}_2$•DITFB**.
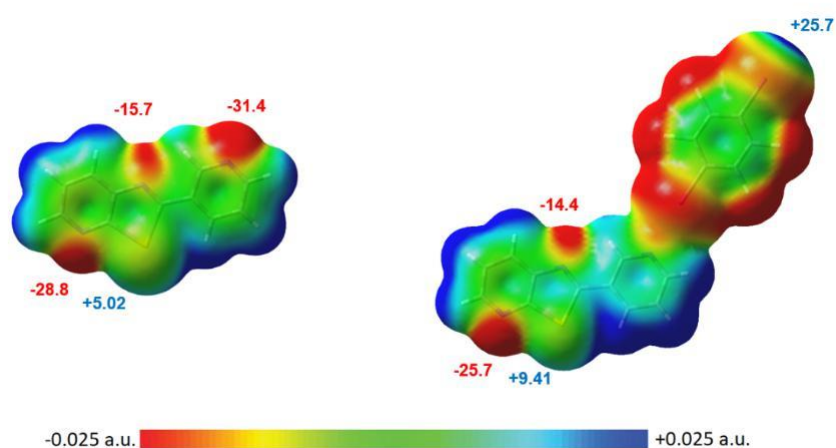
Figure 13. ESP map of molecule **2$^{\text{Se}}$** alone (left) and with **DITFB** through XBI (right). Level of theory: B97D3/Def2-TZVP using Gaussian09 including D01 revision.

The ESP maps of **2$^{\text{Se}}$** and **1$^{\text{Se}}$** (Fig. 13) show that the pyrid-3-yl isomer displays s-hole(a) with a smaller $V_{\text{s,max}}$ value than that of the pyrid-4-yl congener (+5.02 kcal mol^{-1} and +7.09 kcal mol^{-1}, respectively). Upon interaction with **DITFB**, an increase of 4 kcal mol^{-1} is observed for the s-hole(a) (+9.41 kcal mol^{-1} and +11.3 kcal mol^{-1}, respectively), which is too weak to trigger any EBIs.

Solid-state supramolecular polymers with Te-CGP bearing halogen-bond donors. Moving to the CGP derivative substituted with 4-iodo-tetrafluorophenyl, co-crystal $5^{Te}_2 \bullet DABCO$ was obtained as two polymorphs with space groups P" (A) and $P2_1/n$ (B) under the same crystallisation conditions.
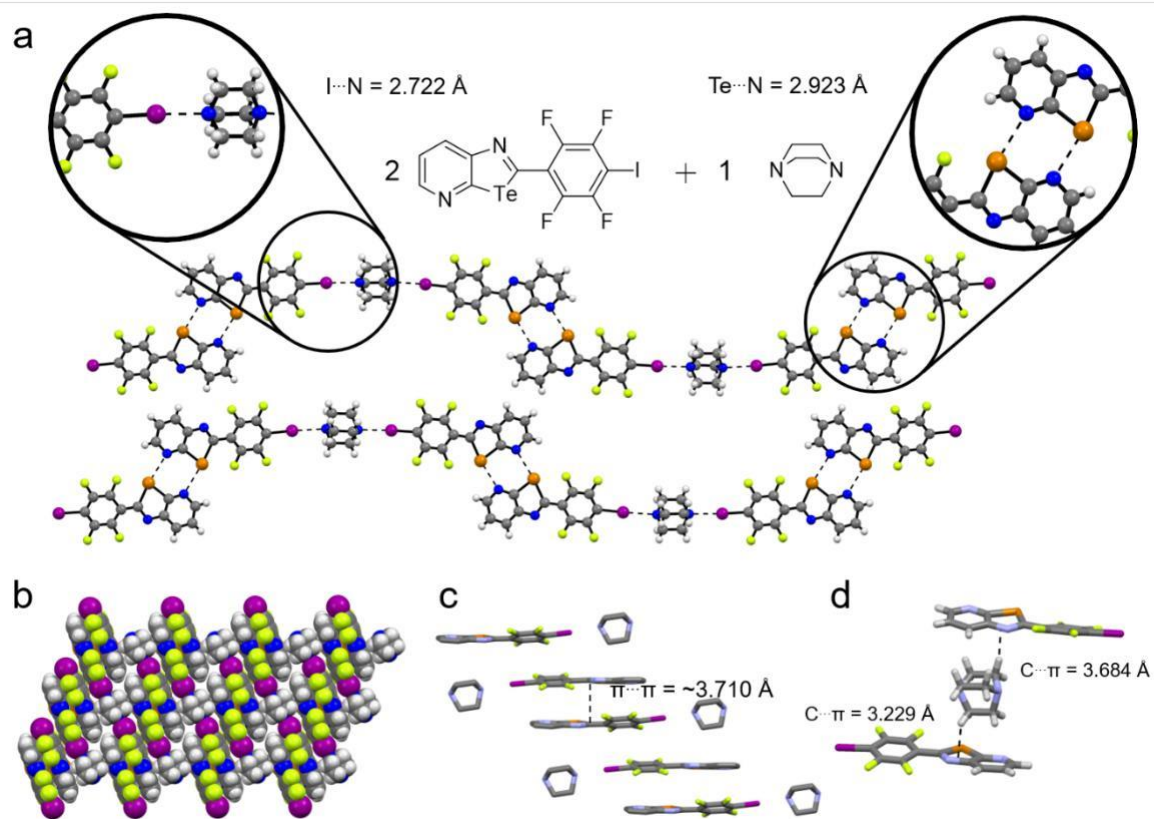
Figure 14. X-ray structure of co-crystal $5^{Te}_2 \bullet DABCO$ as polymorph A. a) Supramolecular polymer and key SBIs; b) vdW sphere representation of the layered organization; c-d) p-p stacking and CH-p interaction. Space group: P". Atom colors: blue N, ocher Te, yellow F, pink I, gray C.

In polymorph A (Fig. 14), 5^{Te} dimerizes through double EBIs ($d_{N...Te}$ = 2.923 Å), with the complexes bridged into a supramolecular polymer through XB bonds ($d_{N...I}$ = 2.722 Å) with **DABCO** linkers. Molecules 5^{Te} p-p stack in a quasi-parallel head-to-tail fashion

(estimated d$_{p-p}$ = 3.710 Å, Fig. 14b-c). **DABCO** molecules are sandwiched between two CGP moieties through CH-p interactions (d$_{C...N}$ = 3.229-3.684 Å, Fig. 15d).
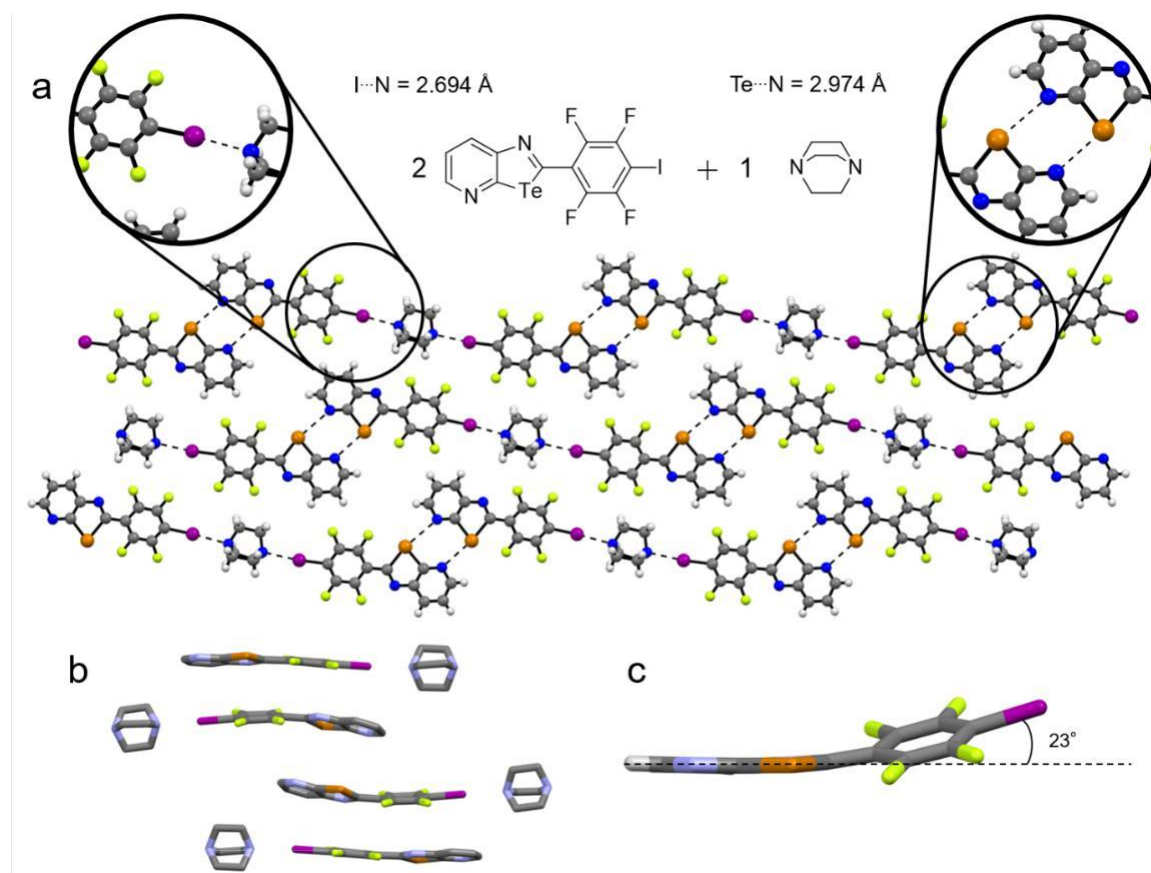
Figure 15. X-ray structure of co-crystal **5Te$_2$•DABCO** as polymorph B. a) Supramolecular polymer and key SBIs; c) p-p stacking and CH-p interactions; c) disorted **5Te** . Space group: P2$_1$/n. Atom colors: blue N, ocher Te, yellow F, pink I, gray C.

Polymorph B of **5Te$_2$•DABCO** was also obtained (Fig. 15), in which molecule **5Te** interacts through double EBIs (d$_{N...Te}$ = 2.974 Å) to form **(5Te)$_2$** units, and a **DABCO** linker is sandwiched between dimers through XBIs (d$_{N...I}$ = 2.694 Å). Notably, one Te-CGP molecule in the asymmetric unit is distorted, with a deviation from the planarity of 23°. While polymorph A was obtained only once,

polymorph B could be reproducibly obtained under the crystallisation conditions described above.
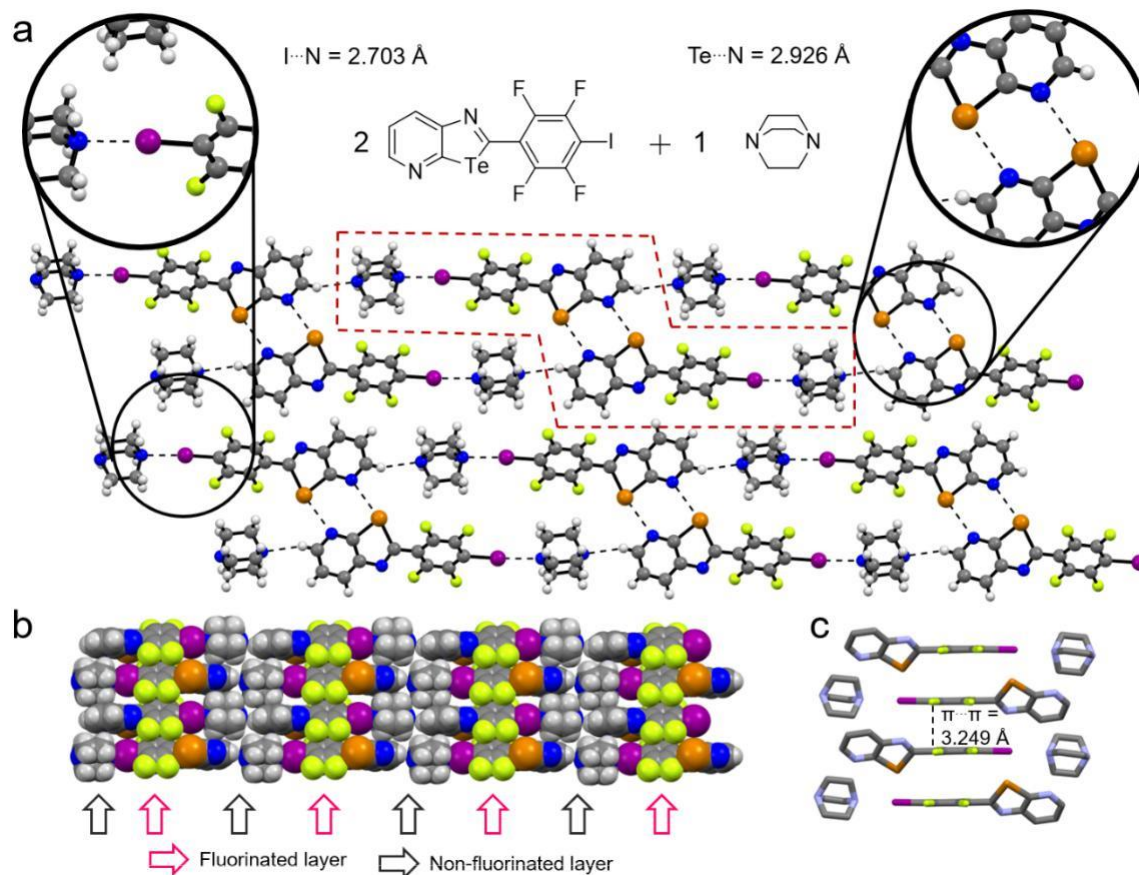
**Figure 16.** X-ray structure of co-crystal **5Te•DABCO**. a) Supramolecular polymer and key SBIs; b) vdW sphere representation of the layered organization; c) p-p stacking interactions. Space group: P$^{"}$. Atom colors: blue N, ocher Te, green F, pink I, gray C.

On the other hands, when growing co-crystals from mixtures containing a 1:10 ratio of **5Te** and **DABCO**, co-crystal **5Te•DABCO** could be obtained. The two components arrange into tetrameric units (Fig. 16, contoured with a red dashed line) where the two central CGP moieties interact through double EBIs (d$_{N...Te}$ = 2.926 Å) and the **DABCO** through XBIs (d$_{N...I}$ = 2.703 Å). As observed for

27

5Te₂•DABCO, also in this case the molecules undergo π-π stacking organization (π-π = 3.289 Å), segregating the synthons into fluorinated (indicated by pink arrows) and non-fluorinated (indicated by grey arrows) domains (Fig. 16b).

At last, when mixing molecules **1ᵀᵉ** and **5ᵀᵉ**, supramolecular polymer **1ᵀᵉ•5ᵀᵉ** was obtained (Fig. 17). Notably, heteromolecular dimers are formed between molecules **1ᵀᵉ** and **5ᵀᵉ** through distorted double EBIs ($d_{N…Te}$ = 3.033 Å, the two CGP moieties sit on planes forming an angle of 33°). In turn, the dimers interact through XBIs ($d_{N…I}$ = 2.802 Å) in a linear fashion (C-I⋯N angle = 172°), forming a polymeric structure. Interestingly, the supramolecular polymer **(1ᵀᵉ•5ᵀᵉ)₂** arranges in a triple-helix structure (Fig. 17b).
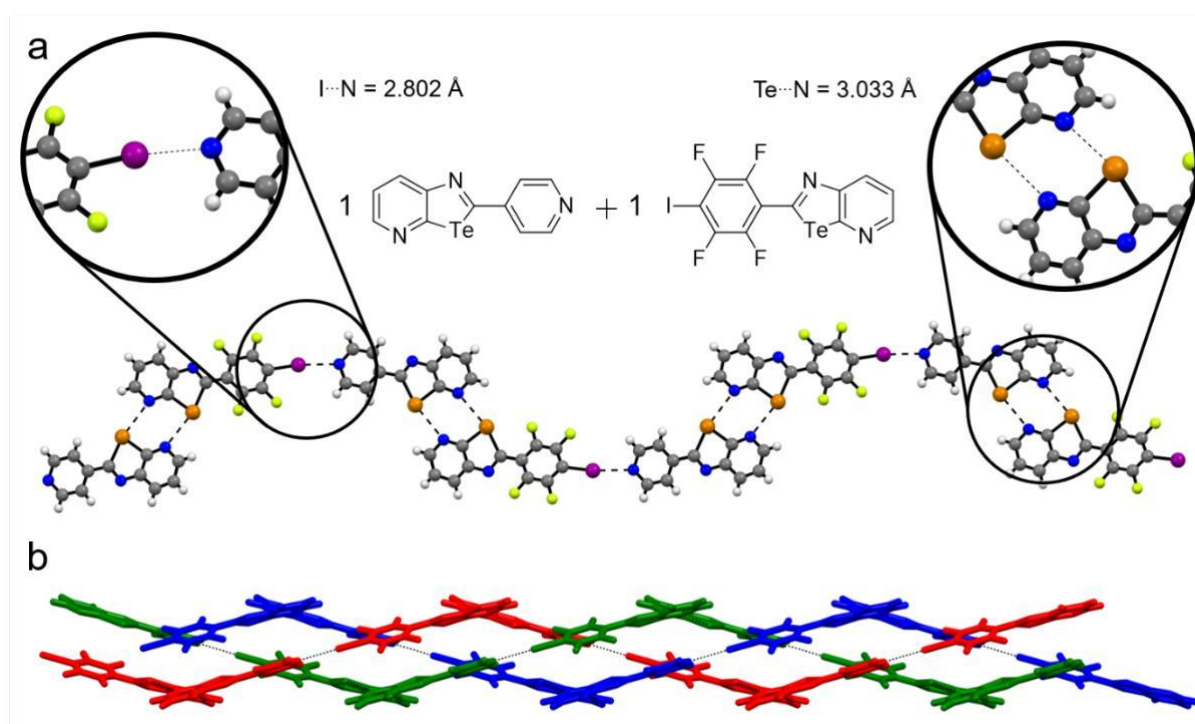
Figure 19. X-ray structure of co-crystal **1ᵀᵉ•5**. a) Supramolecular polymer and key SBIs; b) capped stick representation of the triple helix. Space group: P2₁/n. Atom colors: blue N, ocher Te, green F, pink I, gray C.

In addition, molecules of **1Te** and **5Te** interact through quasi-parallel π -π stacking in an antiparallel fashion (Fig. S23). Both the electron deficient 4-iodotetrafluorophenyl and pyrid-4-yl groups interact with the CGP moiety (ESP maps are provided to indicate the charge distribution).

Conclusions.

In summary, we have demonstrated the possibility to form supramolecular polymers at the solid-state exploiting the simultaneous expression of both XBIs and EBIs. Capitalizing on a preliminary study previusly reported by us using the chalcogen-bonding CGP recognition motif,[23b] in this work we have programmed molecular modules with either a halogen bond acceptor or donor that, interacting with suitable complementary building blocks, undergo the formation of wire-like assemblies at the solid state. In the majority of the solids, both XBIs and EBIs take place without interfering with each other. In particular, mixing **1Te** and **DITFB**, different crystals (**(1Te)$_2$•DITFB, 1Te•DITFB, 1Te•(DITFB)$_2$**) could be obtained depending on the solution ratio of the two components. Isomer **2Te** led to the formation of only **(2Te)$_2$•DITFB**, independently on the initial ratio of the two components. Interestingly, when reference benzotellurazole **3** is used, only halogen-bonding interactions were observed, thus supporting our engineering principle for which the persistency of the CGP recognition motif is crucial to achieve the simultaneous expression of both SBIs. When passing to the Se-

29

CGP modules, molecule **1^{Se}** forms co-crystals with **DITFB**, **(1Te)₂•DITFB**, the strcture of which is similar to that obtained with the Te-containig congener. On the other hand, when using isomer **2^{Se}**, polymers in which the components are held together by HBIs and XBIs have been consinstently obtained. Reversing the Halogen-bonding donating moiety, i.e. adding the electron deficinet halide specie on the CGP, led to the formation of co-crystals **5•DABCO** and **(5)₂•DABCO** in the presence of **DABCO**. At last, when mixing molecules **1Te** and **5**, co-crystal **1Te•5** was obtained. Taken all together, these data further support our idea for which the double chalcogen-bonding interactions established by the CGP moiety is a persistent recognition motif that can be integrated in the design of functional materials.[28] Future challenges would be to apply the principle of using simultaneous XBIs and EBIs to program molecular materials with functional properties and to increase their structural complexity.

Bibliography.

[1]   a) J.-M. Lehn, *Science* **2002**, *295*, 2400-2403; b) J.-M. Lehn, *From Molecular to Supramolecular Chemistry*, Wiley-VCH Verlag GmbH & Co. KGaA, **2006**; c) J.-M. Lehn, *Angew. Chem. Int. Ed.* **2013**, *52*, 2836-2850.

[2]   a) S. J. Rowan, S. J. Cantrill, G. R. L. Cousins, J. K. M. Sanders, J. F. Stoddart, *Angew. Chem. Int. Ed.* **2002**, *41*, 898-952; b) C.-H. Wong, S. C. Zimmerman, *Chem. Commun.* **2013**, *49*, 1679-1695; c) R. J. Sarma, S. Otto, J. R. Nitschke, *Chem. Eur. J.* **2007**, *13*, 9542-9546; d) Z. Rodriguez-Docampo, S. Otto, *Chem. Commun.* **2008**, 5301-5303.

[3]   E. Mattia, S. Otto, *Nat. Nanotechnol.* **2015**, *10*, 111.

[4]   a) P. A. Korevaar, S. J. George, A. J. Markvoort, M. M. J. Smulders, P. A. J. Hilbers, A. P. H. J. Schenning, T. F. A. De Greef, E. W. Meijer, *Nature* **2012**, *481*, 492; b) B. Adelizzi, N. J. Van Zee, L. N. J. de Windt, A. R. A. Palmans, E. W. Meijer, *J. Am. Chem. Soc.* **2019**, *141*, 6110-6121; c) M. J. Webber, E. A. Appel, E. W. Meijer, R. Langer, *Nat. Mater.* **2015**, *15*, 13; d) J.-F. Lutz, J.-M. Lehn, E. W. Meijer, K. Matyjaszewski, *Nat. Rev. Mater.* **2016**, *1*, 16024; e) J.-M. Lehn, *Chem. Soc. Rev.* **2007**, *36*, 151-160; f) J.-M. Lehn, *Prog. Polym. Sci.* **2005**, *30*, 814-831.

[5]   a) N. Roy, B. Bruchmann, J.-M. Lehn, *Chem. Soc. Rev.* **2015**, *44*, 3786-3807; b) T. Aida, E. W. Meijer, S. I. Stupp, *Science* **2012**, *335*, 813; c) S. Dong, Y. Luo, X. Yan, B. Zheng, X. Ding, Y. Yu, Z. Ma, Q. Zhao, F. Huang, *Angew. Chem. Int. Ed.* **2011**, *50*, 1905-1909; d) X. Ji, Y. Yao, J. Li, X. Yan, F. Huang, *J. Am. Chem. Soc.* **2013**, *135*, 74-77.

[6]   a) M. W. Hosseini, *Acc. Chem. Res.* **2005**, *38*, 313-323; b) M. W. Hosseini, *Chem. Commun.* **2005**, 5825-5829; c) M. W. Hosseini, *Coord. Chem. Rev.* **2003**, *240*, 157-166; d) A. Mukherjee, S. Tothadi, G. R. Desiraju, *Acc. Chem. Res.* **2014**, *47*, 2514-2524; e) E. R. T. Tiekink, *Coord. Chem. Rev.* **2017**, *345*, 209-228; f) G. R. Desiraju, *J. Chem. Sci.* **2010**, *122*, 667-675.

[7]   a) W. T. S. Huck, R. Hulst, P. Timmerman, F. C. J. M. van Veggel, D. N. Reinhoudt, *Angew. Chem. Int. Ed.* **1997**, *36*, 1006-1008; b) S.-L. Li, T. Xiao, C. Lin, L. Wang, *Chem. Soc. Rev.* **2012**, *41*, 5950-5968; c) E. Elacqua, D. S. Lye, M. Weck, *Acc. Chem. Res.* **2014**, *47*, 2405-2416.

[8]   a) J. Hermann, R. A. DiStasio, A. Tkatchenko, *Chem. Rev.* **2017**, *117*, 4714-4758; b) H.-J. Schneider, *Angew. Chem. Int. Ed.* **2009**, *48*, 3924-3977; c) M. Ruben, J.-M. Lehn, P. Müller, *Chem. Soc. Rev.* **2006**, *35*, 1056-1067.

[9]   a) H. A. Bent, *Chem. Rev.* **1968**, *68*, 587-648; b) N. W. Alcock, in *Advances in Inorganic Chemistry and*

Radiochemistry, Vol. 15 (Eds.: H. J. Emeléus, A. G. Sharpe), Academic Press, **1972**, pp. 1-58; c) T. M. Beale, M. G. Chudzinski, M. G. Sarwar, M. S. Taylor, *Chem. Soc. Rev.* **2013**, *42*, 1667-1680; d) Á. M. Montaña, *Chem. Select* **2017**, *2*, 9094-9112; e) M. Fourmigué, P. Batail, *Chem. Rev.* **2004**, *104*, 5379-5418; f) G. Cavallo, P. Metrangolo, T. Pilati, G. Resnati, G. Terraneo, *Cryst. Growth Des.* **2014**, *14*, 2697-2702.

[10] a) P. Metrangolo, G. Resnati, *Science* **2008**, *321*, 918-919; b) L. C. Gilday, S. W. Robinson, T. A. Barendt, M. J. Langton, B. R. Mullaney, P. D. Beer, *Chem. Rev.* **2015**, *115*, 7118-7195; c) M. Erdelyi, *Chem. Soc. Rev.* **2012**, *41*, 3547-3557.

[11] a) K. Raatikainen, J. Huuskonen, M. Lahtinen, P. Metrangolo, K. Rissanen, *Chem. Commun.* **2009**, 2160-2162; b) P. Metrangolo, F. Meyer, T. Pilati, D. M. Proserpio, G. Resnati, *Chem. Eur. J.* **2007**, *13*, 5765-5772; c) C. B. Aakeröy, D. Welideniya, J. Desper, C. Moore, *Cryst. Eng. Comm.* **2014**, *16*, 10203-10209; d) L. Catalano, S. Pérez-Estrada, G. Terraneo, T. Pilati, G. Resnati, P. Metrangolo, M. A. Garcia-Garibay, *J. Am. Chem. Soc.* **2015**, *137*, 15386-15389; e) W. Navarrini, P. Metrangolo, T. Pilati, G. Resnati, *New J. Chem.* **2000**, *24*, 777-780.

[12] a) M. Saccone, M. Spengler, M. Pfletscher, K. Kuntze, M. Virkki, C. Wölper, R. Gehrke, G. Jansen, P. Metrangolo, A. Priimagi, M. Giese, *Chem. Mater.* **2019**, *31*, 462-470; b) H. L. Nguyen, P. N. Horton, M. B. Hursthouse, A. C. Legon, D. W. Bruce, *J. Am. Chem. Soc.* **2004**, *126*, 16-17; c) J. Xu, X. Liu, J. K.-P. Ng, T. Lin, C. He, *J. Mater. Chem.* **2006**, *16*, 3540-3545; d) J. Xu, X. Liu, T. Lin, J. Huang, C. He, *Macromolecules* **2005**, *38*, 3554-3557; e) N. Houbenov, R. Milani, M. Poutanen, J. Haataja, V. Dichiarante, J. Sainio, J. Ruokolainen, G. Resnati, P. Metrangolo, O. Ikkala, *Nat. Commun.* **2014**, *5*, 4043; f) J. Vapaavuori, A. Siiskonen, V. Dichiarante, A. Forni, M. Saccone, T. Pilati, C. Pellerin,

A. Shishido, P. Metrangolo, A. Priimagi, *RSC Adv.* **2017**, 7, 40237-40242.

[13] a) A. Priimagi, G. Cavallo, P. Metrangolo, G. Resnati, *Acc. Chem. Res.* **2013**, *46*, 2686-2695; b) C. B. Aakeröy, T. K. Wijethunga, J. Benton, J. Desper, *Chem. Commun.* **2015**, *51*, 2425-2428; c) W. Zhu, R. Zheng, Y. Zhen, Z. Yu, H. Dong, H. Fu, Q. Shi, W. Hu, *J. Am. Chem. Soc.* **2015**, *137*, 11038-11046; d) M. Virkki, O. Tuominen, A. Forni, M. Saccone, P. Metrangolo, G. Resnati, M. Kauranen, A. Priimagi, *J. Mater. Chem. C* **2015**, *3*, 3003-3006; e) M. Saccone, V. Dichiarante, A. Forni, A. Goulet-Hanssens, G. Cavallo, J. Vapaavuori, G. Terraneo, C. J. Barrett, G. Resnati, P. Metrangolo, A. Priimagi, *J. Mater. Chem. C* **2015**, *3*, 759-768; f) J. Vapaavuori, I. T. S. Heikkinen, V. Dichiarante, G. Resnati, P. Metrangolo, R. G. Sabat, C. G. Bazuin, A. Priimagi, C. Pellerin, *Macromolecules* **2015**, *48*, 7535-7542; g) A. Priimagi, G. Cavallo, A. Forni, M. Gorynsztejn-Leben, M. Kaivola, P. Metrangolo, R. Milani, A. Shishido, T. Pilati, G. Resnati, G. Terraneo, *Adv. Funct. Mater.* **2012**, *22*, 2572-2579; h) F. Meyer, P. Dubois, *Cryst. Eng. Comm.* **2013**, *15*, 3058-3071; i) P. Liu, Z. Li, B. Shi, J. Liu, H. Zhu, F. Huang, *Chem. Eur. J.* **2018**, *24*, 4264-4267.

[14] a) M. Cametti, B. Crousse, P. Metrangolo, R. Milani, G. Resnati, *Chem. Soc. Rev.* **2012**, *41*, 31-42; b) P. Metrangolo, G. Resnati, *Nat. Chem.* **2012**, *4*, 437-438.

[15] a) C. Cohen-Addad, M. S. Lehmann, P. Becker, L. Parkanyi, A. Kalman, *J. Chem. Soc., Perkin Trans. 2* **1984**, 191-196; b) C. Bleiholder, D. B. Werz, H. Köppel, R. Gleiter, *J. Am. Chem. Soc.* **2006**, *128*, 2666-2674; c) A. F. Cozzolino, P. J. W. Elder, I. Vargas-Baca, *Coord. Chem. Rev.* **2011**, *255*, 1426-1438; d) J. Fanfrlik, A. Prada, Z. Padelkova, A. Pecina, J. Machacek, M. Lepsik, J. Holub, A. Ruzicka, D. Hnyk, P. Hobza, *Angew. Chem. Int. Ed.* **2014**, *53*, 10139-10142; e) R. E. Rosenfield, Jr., R. Parthasarathy, J. D. Dunitz, *J. Am. Chem. Soc.* **1977**, *99*, 4860-4862; f) D. J. Pascoe, K. B. Ling,

S. L. Cockroft, *J. Am. Chem. Soc.* **2017**, *139*, 15160-15167; g) K. T. Mahmudov, M. N. Kopylovich, M. F. C. Guedes da Silva, A. J. L. Pombeiro, *Dalton Trans.*, **2017**, *46*, 10121-10138; h) W. Wang, B. Ji, Y. Zhang, *J. Phys. Chem. A*, **2009**, *113*, 8132-8135; i) L. Brammer, *Faraday Discuss.*, **2017**, *203*, 485-507; l) A. F. Cozzolino, I. Vargas-Baca, S. Mansour, A. H. Mahmoudkhani, *J. Am. Chem. Soc.* **2005**, *127*, 3184-3190.

[16] For selected review in the field: a) A. Bauzá, D. Quiñonero, P. M. Deyà, A. Frontera, *CrystEngComm*, **2013**, 15, 3137-3144; b) P. Scilabra, G. Terraneo, G. Resnati, *Acc. Chem. Res.* **2019**, *52*, 1313-1324; selected examples in the field: c) D. B. Werz, Rolf Gleiter, F. Rominger, *J. Am. Chem. Soc.*, **2002**, *124*, 10638-10639; d) J. Fanfrlík, A. Přáda, Z. Padělková, A. Pecina, J. Macháček, M. Lepšík, J. Holub, A. Růžička, D. Hnyk, P. Hobza, *Angew. Chem. Int. Ed.* **2014**, *53*, 10139-10142; e) A. Kremer, A. Fermi, N. Biot, J. Wouters, D. Bonifazi, *Chem. Eur. J.* **2016**, *22*, 5665-5675; f) F. Di Maria, P. Olivelli, M. Gazzano, A. Zanelli, M. Biasiucci, G. Gigli, D. Gentili, P. D'Angelo, M. Cavallini, G. Barbarella, *J. Am. Chem. Soc.*, **2011**, *133*, 8654-8661; g) R. Neidlein, D. Knecht, H. Endres, *Zeitschrift für Naturforschung B* **1987**, *42*, 84; h) T. Chivers, X. Gao, M. Parvez, *Inorg. Chem.* **1996**, *35*, 9-15; i) A. F. Cozzolino, J. F. Britten, I. Vargas-Baca, *Cryst. Growth Des.* **2006**, *6*, 181-186.

[17] a) S. Benz, M. Macchione, Q. Verolet, J. Mareda, N. Sakai, S. Matile, *J. Am. Chem. Soc.* **2016**, *138*, 9093-9096; b) G. E. Garrett, E. I. Carrera, D. S. Seferos, M. S. Taylor, *Chem. Commun.* **2016**, *52*, 9881-9884; c) G. E. Garrett, G. L. Gibson, R. N. Straus, D. S. Seferos, M. S. Taylor, *J. Am. Chem. Soc.* **2015**, *137*, 4126-4133; d) J. Y. C. Lim, I. Marques, A. L. Thompson, K. E. Christensen, V. Félix, P. D. Beer, *J. Am. Chem. Soc.* **2017**, *139*, 3122-3133.

[18] a) S. Benz, J. López-Andarias, J. Mareda, N. Sakai, S. Matile, *Angew. Chem. Int. Ed.* **2017**, *56*, 812-815; b) P. Wonner, L. Vogel, M. Düser, L. Gomes, F. Kniep, B. Mallick,

D. B. Werz, S. M. Huber, *Angew. Chem. Int. Ed.* **2017**, *56*, 12009-12012; c) S. Benz, J. Mareda, C. Besnard, N. Sakai, S. Matile, *Chem. Sci.* **2017**, *8*, 8164-8169.

[19] a) M. Giroud, J. Ivkovic, M. Martignoni, M. Fleuti, N. Trapp, W. Haap, A. Kuglstatter, J. Benz, B. Kuhn, T. Schirmeister, F. Diederich, *ChemMedChem* **2016**, 12, 257-270; b) D. Manna, G. Mugesh, *J. Am. Chem. Soc.* **2012**, 134, 4269-4279.

[20] a) Peter C. Ho, P. Szydlowski, J. Sinclair, P. J. W. Elder, J. Kübel, C. Gendy, L. Myongwon Lee, H. Jenkins, J. F. Britten, D. R. Morim, I. Vargas-Baca, *Nature Commun.* **2016**, 7, 11299; b) P. C. Ho, R. Bui, A. Cevallos, S. Sequeira, J. F. Britten, I. Vargas-Baca, *Dalton Trans.*, **2019**, *48*, 4879-4886; c) L.-J. Riwar, N. Trapp, K. Root, R. Zenobi, F. Diederich, *Angew. Chem. Int. Ed.* **2018**, *57*, 17259-17264; d) M. R. Ams, N. Trapp, A. Schwab, J. V. Milić, F. Diederich, *Chem. Eur. J.* **2018**, *25*, 323-333; e) K. Strakova, L. Assies, A. Goujon, F. Piazzolla, H. V. Humeniuk, S. Matile, *Chem. Rev.* **2019**, *119*, 10977-11005; f) A. F. Cozzolino, I. Vargas-Baca, *J. Organomet. Chem.* **2007**, *692*, 2654-2657.

[21] a) S. Zhu, C. Xing, W. Xu, G. Jin, Z. Li, *Cryst. Growth Des.* **2004**, *4*, 53-56; b) V. Vasylyeva, S. K. Nayak, G. Terraneo, G. Cavallo, P. Metrangolo, G. Resnati, *Cryst. Eng. Comm.* **2014**, *16*, 8102-8105; c) A. R. Voth, P. Khuu, K. Oishi, P. S. Ho, *Nat. Chem.* **2009**, *1*, 74.

[22] a) E. Persch, O. Dumele, F. Diederich, *Angew. Chem. Int. Ed.* **2015**, *54*, 3290-3327; b) P. Auffinger, F. A. Hays, E. Westhof, P. S. Ho, *Proc. Natl. Acad. Sci. U.S.A* **2004**, *101*, 16789.

[23] a) K. Eichstaedt, A. Wasilewska, B. Wicher, M. Gdaniec, T. Połoński, *Cryst. Growth Des.* **2016**, *16*, 1282-1293; b) N. Biot, D. Bonifazi, *Chem. Eur. J.* **2018**, *24*, 5439-5443; c) Y. V. Torubaev, D. K. Rai, I. V. Skabitsky, S. Pakhira, A. *New J. Chem.* **2019**, *43*, 7941-7949.

[24] Y. Lu, W. Li, W. Yang, Z. Zhu, Z. Xu, H. Liu, *Phys. Chem. Chem. Phys.*, **2019**, *21*, 21568.

[25] a) P. Metrangolo, F. Meyer, T. Pilati, G. Resnati, G. Terraneo, *Angew. Chem. Int. Ed.* **2008**, *47*, 6114-6127; b) M. Fourmigué, *Curr. Opin. Solid State Mater. Sci.* **2009**, *13*, 36-45; c) P. Metrangolo, G. Resnati, *Chem. Eur. J.* **2001**, *7*, 2511-2519; d) R. Cabot, C. A. Hunter, *Chem. Commun.* **2009**, 2005-2007.

[26] A. Kremer, C. Aurisicchio, F. De Leo, B. Ventura, J. Wouters, N. Armaroli, A. Barbieri, D. Bonifazi, *Chem. Eur. J.* **2015**, *21*, 15377-15387.

[27] a) T. Clark, M. Hennemann, J. S. Murray, P. Politzer, *J. Mol. Model.* **2007**, *13*, 291-296; b) J. S. Murray, P. Lane, P. Politzer, *Int. J. Quantum Chem.* **2007**, *107*, 2286-2292; c) P. Politzer, J. S. Murray, P. Lane, *Int. J. Quantum Chem.* **2007**, *107*, 3046-3052; d) P. Politzer, J. S. Murray, T. Clark, *Phys. Chem. Chem. Phys.* **2013**, *15*, 11178-11189.

[28] For some examples of materials application of XBIs see: a) K. Jie, Y. Zhou, E. Li, Z. Li, R. Zhao, F. Huang, *J. Am. Chem. Soc.* **2017**, *139*, 15320-15323; b) B. Shi, L. Shangguan, H. Wang, H. Zhu, H. Xing, P. Liu, Y. Liu, J. Liu, F. Huang, *ACS Mat. Lett.* **2019**, *1*, 111-115.